

Developing Dynamic Killing Technique for Off-Bottom Killing Condition

Mohamed Yossef*, Belayim Petroleum Company, Cairo, Egypt; **Adel Salem**, Suez University, Suez, Egypt and Future University in Egypt (FUE), Cairo, Egypt

Abstract

Dynamic killing is a non-conventional well control technique that employs annular pressure loss in conjunction with hydrostatic pressure to halt well influx. This method is particularly applicable in off-bottom conditions, where the drill bit is away from the well's bottom. Off-bottom conditions are common during tripping operations, where surface pressure may not accurately reflect bottom-hole conditions. Ignoring the region beneath the drill bit necessitates higher kill rates, which may exceed equipment limits, such as maximum rated surface pressure.

In this study, the effect of kill fluid falling below the drill bit was examined in terms of critical influx velocity. A Python program was developed to model single-phase and two-phase flow conditions within the drill string, annulus, and below the bit. The focus was on accurately modeling the area below the bit, using three different approaches: static, dynamic zero net liquid holdup (ZNLH) flow, and countercurrent two-phase flow.

Two gas influx scenarios were employed to test, verify, and assess these modeling approaches. Results indicated that the static ZNLH approach required the highest kill rate, while the countercurrent two-phase flow approach required the lowest. In terms of bottom-hole pressure, the static ZNLH approach resulted in the lowest pressures, whereas the countercurrent two-phase flow approach yielded the highest pressures.

Temperature significantly impacts the properties of the kill fluid, such as density and viscosity, even when water is used. Additionally, reducing the kill string depth logarithmically increases the required kill rate. The critical gas velocity, which influences the kill fluid's fall-off at a certain depth, decreases with increasing gas influx rate. This work provides a roadmap for applying dynamic kill techniques in off-bottom conditions, accommodating both low and high gas influx rates.

Introduction

The conventional well control techniques based on the constant bottom hole pressure (BHP) concept in some cases fails to control well kicks. From well's blowout statistics, 25% of blowouts happened due to swabbing effect due to excessive tripping speed while pull out of hole. Meanwhile 80% of blowout events happened when the bit position is off-bottom in those cases the dynamic kill technique incorporated (Yin et al. 2023). The dynamic kill method, announced by Mobil Oil Corporation and initially presented by Blount and Soeiinah, was used to control a high-deliverability gas well blowout (400 MMscf/day) in Indonesia's Arun Field, which continued to burn for 89 days. The blowout was controlled within 50 minutes once the killing operation commenced (Vallejo-Arrieta 2002).

Copyright © the author(s). This work is licensed under a Creative Commons Attribution 4.0 International License.

Improved Oil and Gas Recovery

DOI: 10.14800/IOGR.1291

Received July 2, 2024; revised August 14, 2024; accepted August 20, 2024.

*Corresponding author: mahamadaya_184@yahoo.com

The dynamic kill technique involves pumping fluid at the surface into the blowout flow path to increase the combined annular pressure loss and hydrostatic pressure along the blowout flow path, surpassing the formation pressure. In some instances, blowouts occur while the drill string remains off-bottom, complicating the well-killing process as the ability to circulate the kick fluid out is not feasible.

Limited research has been conducted on off-bottom kills, particularly considering the ability of heavier kill fluid to fall and flow counter-current against the formation fluid, which supports well killing.

This paper aims to simulate the off-bottom dynamic kill process for gas well blowouts, highlighting the effect of liquid fall-down on selecting the killing rate. The study incorporates different flow models, including two-phase flow models, static zero net liquid holdup, and dynamic zero net liquid holdup, to achieve a more accurate flow model for calculating well-killing requirements.

The counter-current flow of killing fluid dropping through the influx fluid was primarily studied by Gillespie et al. (1990) for off-bottom dynamic killing conditions. They defined a certain limit at which the kill fluid begins to fall through the gas influx, termed the critical gas velocity. This is defined as the gas velocity at which the liquid begins to fall, considered equal to the relative settling velocity of the largest droplet. The critical gas velocity variables are illustrated in **Eq. 1** (Gillespie et al. 1990). They based the well-killing condition on two variables: the largest droplet diameter in the gas stream and the droplet drag coefficient.

$$v_{Scrit} = \sqrt{\frac{4g d_{max}(\rho_l - \rho_g)}{3\rho_g K_d}}, \dots\dots\dots(1)$$

Gillespie et al. (1990) used three approaches for droplet size estimation, which produced different critical velocity values, varying widely, with the highest value being almost four times the lowest for the same conditions. A high value for the droplet drag coefficient would lead to a conservative estimate of the critical gas velocity (Gillespie et al. 1990; Flores-Avila et al. 2003). Additionally, liquid holdup, which may exist while circulating a fluid, was not considered in their estimation.

Kouba et al. (1993) employed the critical gas velocity model to estimate formation fluid rates below which a minimum value of liquid holdup would exist. They utilized Barnea's studies, which indicated that liquid holdup is 0.25 during slug flow, 0.75 for bubble flow, and zero for annular flow, to estimate the liquid holdup below the killing string during off-bottom dynamic killing operations. They made several assumptions: no-slip flow between the gas and liquid phases above the injection point, no friction pressure loss below the injection point, and a minimum value of liquid holdup for each flow pattern. These assumptions led to higher required kill rates (Kouba et al. 1993; Flores-Avila et al. 2003).

Flores-Avila et al. (2002) extended the research on the effect of kill fluid falling through the upward-moving formation kick fluid, particularly when the injection point is off-bottom in blowout wells. Their study demonstrated that the accumulation of injected kill fluid below the kill string would increase bottom hole pressure and assist in killing the well by using two important concepts.

The first concept is the critical gas velocity, which controls the accumulation of kill fluid below the injection point. This was predicted by revising Turner's (Turner et al. 1969) model of terminal velocity for liquid droplets. The new proposed model considers the flow regime of the continuous phase when evaluating the drag coefficient, suggesting a value of 0.44 instead of the 0.2 proposed by Turner et al. (1969). Additionally, they incorporated the deviation angle from the vertical, as given by **Eq. 2** (Flores-Avila et al. 2003).

$$v_{Scrit} = 14.27 \left(\sigma \frac{\rho_l - \rho_g}{K_d \cos \alpha \rho_g^2} \right)^{0.25}, \dots\dots\dots(2)$$

The second concept is the volume of kill fluid that falls and accumulates below the injection point, which can be predicted using the concept of static Zero Net Liquid Flow holdup (ZNLFF).

Zero Net Liquid Flow Hold-up. Liquid hold-up is defined as the ratio of the liquid volume in a pipe portion to the total volume of that portion under downhole conditions. Conversely, the zero net liquid flow (ZNLf) hold-up expression arises when a portion of a well becomes filled with dropped liquid while gas flows through that well portion, rendering the liquid portion stagnant (Flores-Avila et al. 2002).

Typically, slip velocity is the difference between the absolute velocities of the gas and liquid phases. The absolute velocity is defined as the ratio between superficial velocity and its volumetric hold-up, as given in **Eq. 3**. However, under vertical ZNLf conditions, the liquid is stagnant, resulting in a superficial liquid velocity of zero. Thus, ZNLf is defined by **Eq. 4** (Kanshio 2019):

$$v_s = v_g - v_l = \frac{v_{sg}}{(1-H_l)} - \frac{v_{sl}}{H_l} \dots\dots\dots(3)$$

$$v_{G0} = \frac{v_{sg}}{(1-H_{l0})} \dots\dots\dots(4)$$

Where,

$$H_{l0} = 1 - \frac{v_{sg}}{v_{G0}} \dots\dots\dots(5)$$

Flores-Avila et al. (2002) utilized the experimental results of Arpandi et al. (1996), which were conducted for a gas-liquid cylindrical cyclone with multiphase inlet flow and continuous liquid phase withdraw from vessel bottom and gas exit from top as explained in **Figure 1**, to calculate gas slip velocity (**Eq. 6**) and, consequently, the zero net liquid flow (**Eq. 7**).

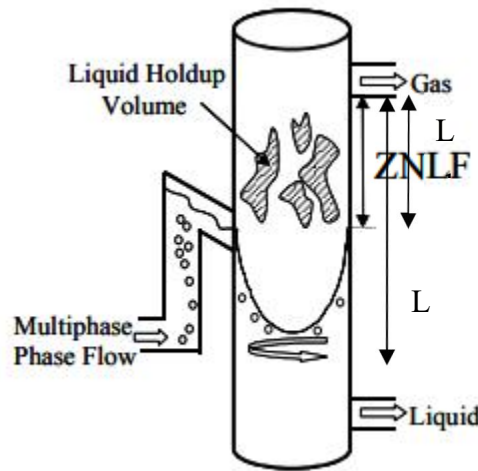


Figure 1—Gas-liquid cylindrical cyclone (Flores-Avila et al. 2003).

$$v_{G0} = 1.15 v_{sg} + 0.35 \sqrt{\frac{g d_i (\rho_l - \rho_g)}{3 \rho_g K_d}} \dots\dots\dots(6)$$

$$H_{l0} = [1 - \frac{v_{sg}}{v_{G0}}] (1 - \frac{L_d}{L_p}) \dots\dots\dots(7)$$

Enhanced Model

In this study, we aimed to develop an enhanced model to account for the effect of liquid fall-off below the kill string. The dynamic kill mathematical model was established to evaluate the killing process in off-bottom scenarios. The model consists of two major components: the reservoir inflow performance model and the wellbore performance model. Combining these models provides the actual well blowout deliverability, which serves as the starting point for the modeling process.

The model divides the well system into four distinct regions, as illustrated in **Figure 2**. *Region 1* represents the formation, which is the source of the blowout fluid flow. *Region 2*, located in the wellbore, encompasses the section where counter-current two-phase flow occurs, with upward-moving formation fluid and downward-moving kill fluid, starting from the end of the kill string to the bottom of the well. *Region 3*, also within the wellbore, represents co-current two-phase flow, where both formation and kill fluids move upward through the annulus from the end of the kill string depth to the surface. Finally, *Region 4* is characterized by single-phase flow, with kill fluid moving downward inside the kill string.

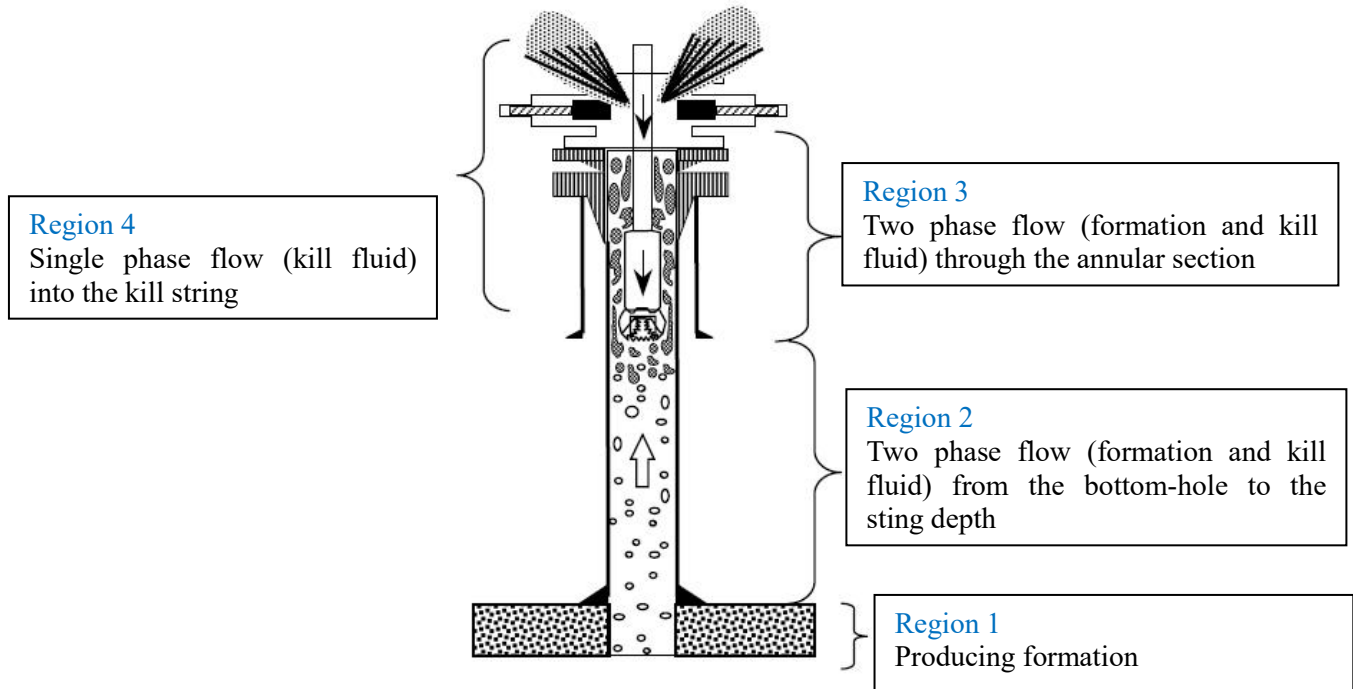


Figure 2—Off-bottom well blowout system modeling with four regions (Vallejo-Arrieta 2002).

Reservoir Model (Region 1). The reservoir model was constructed using Forchheimer’s equation (**Eq. 8**) for radial gas flow in porous media. This model accounts for high gas velocities near the wellbore by incorporating a non-Darcy gas flow term, as described in **Eq. 11** (Ikoku 1980; Forchheimer 1901).

$$P_R^2 - P_{wf}^2 = A Q_{sc} + B Q_{sc}^2, \dots\dots\dots(8)$$

Where,

$$B = \frac{1422 \mu_g z_r T_r}{k h} \left[\ln \left(0.472 \frac{r_e}{r_w} \right) \right], \dots\dots\dots(9)$$

$$A = \frac{3.161 \cdot 10^{-12} \beta Y_g z_r T_r}{h^2} \left(\frac{1}{r_e} - \frac{1}{r_w} \right), \dots\dots\dots(10)$$

$$\beta = \frac{2.33 \cdot 10^{10}}{k_g^{1.201}}, \dots\dots\dots(11)$$

Wellbore Model. The wellbore model is based on the general conservation equation and Newton’s second law to derive the general form of the pressure gradient, as shown in **Eq. 12**. This implies that the total pressure loss across the system is the sum of pressure losses due to hydrostatic pressure reduction, friction loss caused by the

shearing force between the fluid and the pipe wall, and pressure loss due to fluid acceleration. The acceleration component is typically negligible due to its minor effect on the total pressure loss value.

$$\left(\frac{dP}{dL}\right)_{\text{total}} = \left(\frac{dP}{dL}\right)_{\text{elevation}} + \left(\frac{dP}{dL}\right)_{\text{friction}} + \left(\frac{dP}{dL}\right)_{\text{acceleration}} \dots \dots \dots (12)$$

To enhance the model's accuracy, the effect of temperature changes was incorporated by using the wellbore temperature model proposed by Hassan and Kabir, as detailed in **Eq. 13** (Hassan and Kabir 2012; Hasan and Kabir 2018),

$$T_{ann} = T_{ei} + \frac{1 - e^{-(\alpha - l) L_R}}{L_R} \left(g_G \sin \alpha - \frac{g_G \sin \alpha}{C_p J g} \right) \dots \dots \dots (13)$$

Single Phase Flow (Region 4). In this region, which contains only killing fluid, sea water is used due to the large volume required for the dynamic killing process, making water a practical choice. Therefore, the general pressure gradient equation for this region can be expressed as shown in **Eq. 14** (in field units),

$$\left(\frac{dP}{dL}\right)_{\text{total}} = \left(\frac{\rho_l}{144}\right) + \left(\frac{\rho_l f v_l^2}{772.17 D_s}\right) \dots \dots \dots (14)$$

Concurrent Two-phase Flow (Region 3). This region features concurrent flow, where both kill fluid (water) and reservoir fluid (gas) move in the same direction (upward) through the annulus, from the end of the drill string to the surface. In a two-phase flow scenario, the flow regime transitions through several stages: annular flow, churn flow, slug flow, and ultimately bubble flow as the liquid hold-up reaches its maximum value.

To model this flow condition, the mechanistic two-phase flow model presented by Hassan and Kabir (2007) was employed. This model establishes specific conditions to identify the flow regime. Once the flow type is detected, flow parameters are determined from **Table 1**, and the nature of gas bubble rise velocity is selected. At this stage, **Eq. 15** can be used to calculate the gas void fraction (H_g).

$$H_g = \frac{v_{sg}}{C_o v_m + v_{\infty}} \dots \dots \dots (15)$$

Table 1—Flow parameter according flow pattern and type.

Flow pattern	Flow parameter, C_o		Gas rise velocity, v_{∞}
	Concurrent upward	Countercurrent	
Bubble	1.2	2.0	$v_{\infty b}$
Slug	1.2	1.2	v_{∞}
Churn	1.15	1.15	v_{∞}
Annular	1.0	1.0	0

For the two-phase flow, mixture fluid parameters are computed based on the volumetric weighted average for the two phases, as illustrated in **Eqs. 16 through 19**.

$$H_l = 1 - H_g \dots \dots \dots (16)$$

$$\rho_m = \rho_l H_l + \rho_g H_g \dots \dots \dots (17)$$

$$\rho_m = \rho_l H_l + \rho_g H_g \dots \dots \dots (18)$$

$$\mu_m = \mu_l H_l + \mu_g H_g \dots \dots \dots (19)$$

Countercurrent Two-phase Flow (Region 2). Region 2 is crucial in the off-bottom dynamic kill model, as it examines how the area below the kill string affects the required dynamic kill rate. This area is often neglected, but if the kill fluid coming out from the kill string falls down to the bottom of the well in the opposite direction

to the kicked fluid, it will contribute to the well-killing process. If the gas superficial velocity at the end of the kill string is less than the critical velocity, the kill fluid will fall down.

To study this region, two different approaches can be utilized. The first approach involves using the two-phase mechanistic model for countercurrent flow conditions as presented by Hassan and Kabir (2007). In this model, since the two-phase flows are in opposite directions, the void fraction equation is applied with a negative sign, as shown in **Eq. 20**.

$$H_g = \frac{v_{sg}}{C_o v_m - v_{\infty}}, \dots \dots \dots (20)$$

The second approach employs the dynamic zero net liquid hold-up (ZNLH) method to determine the liquid hold-up below the kill string. Kolla et al. (2018) conducted laboratory tests to evaluate the dynamic ZNLH and developed a model that accounts for the fluid properties of both kick and kill fluids, as well as the superficial velocity of the kill fluid. This model is detailed in **Eqs. 21 through 25** (Kolla et al. 2018).

$$v_{Sg}^{*2} + v_{Sl}^{*2} = 1, \dots \dots \dots (21)$$

$$v_{Sg}^* = v_{sg} \rho_g^{0.5} [g D (\rho_l - \rho_g)]^{-0.5}, \dots \dots \dots (22)$$

$$v_{Sl}^* = v_{slz}^{2n} \rho_l^n [g D (\rho_l - \rho_g)]^{-n}, \dots \dots \dots (23)$$

$$n = \left(\frac{25 \mu \sqrt{g D}}{\sigma} \right)^{0.25}, \dots \dots \dots (24)$$

$$H_{LDZ} = \frac{v_{slz}}{(v_{slz} + v_{sg})}, \dots \dots \dots (25)$$

Model Verification. To assess the accuracy of the model, its results were validated against actual well blowout and killing data from Indonesia's Arun Field (Kouba et al. 1993) and the case analyzed by Gillespie et al. (1990), which involved a potential dynamic kill of a workover well under off-bottom conditions.

Arun Field Blowout. For the Arun Field blowout case, reservoir data and wellbore input data, as detailed in **Table 2**, were used to establish the well flow model. The model output was then compared with the actual data. Initially, the data were used to construct the well's blowout IPR/VLP model, which provided the initial conditions for the well-killing process and resulted in a well blowout rate of 454,000 MMSF/D (**Figure 3**). The same data in **Table 2** were also used to develop the well IPR/VLP performance curve using commercial software (PROSPER), yielding a well blowout rate of 473,841 MMSF/D (**Figure 4** and **Table 3**).

Table 2—Blowout data from Mobil Oil Indonesia's Arun Field well C-II-2.

Input Data	Value
Reservoir pressure (psia)	7,100
Reservoir temperature (°F)	230
Gas specific gravity	0.6
Casing ID (in)	8.535
Drillpipe OD (in)	5.00
Drillpipe ID (in)	4.275
Pipe roughness (in)	0.0018
Measured depth (ft)	10,210
True vertical depth (ft)	9,650

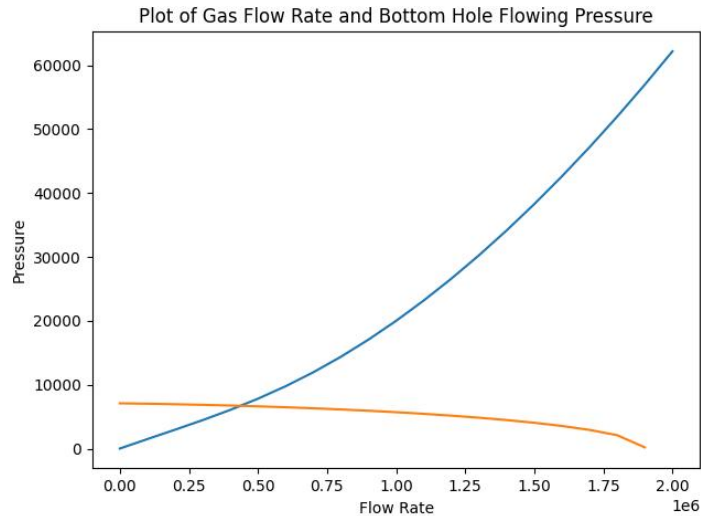


Figure 3—Well's blowout rate using IPR/VLP model.

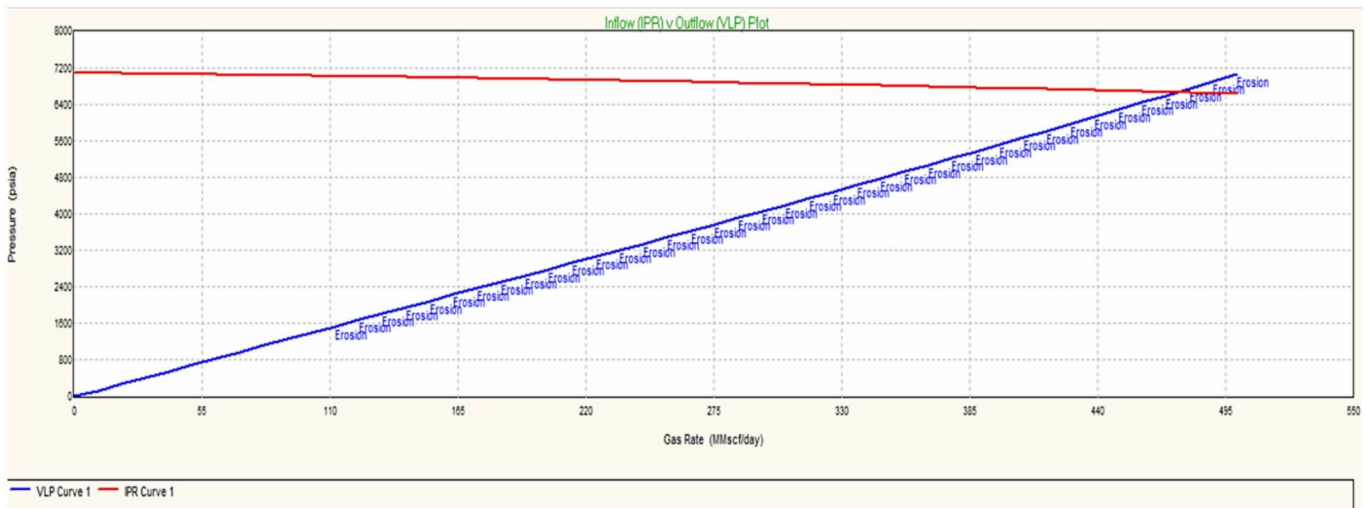


Figure 4—Well's blowout rate using commercial software.

Table 3—Summary of well IPR/VLP performance using commercial software.

Parameters	Values	Units
Gas Rate	473,841	MMscf/day
Oil Rate	0	STB/day
Water Rate	0	STB/day
Liquid Rate	0	STB/day
Solution Node Pressure	6672.51	psia
dP Friction	5947.1	psi
dP Gravity	710.399	psi

Secondly, the verification of the well-killing dynamic model was conducted by comparing the model results for the killing rate of Arun Field well C-II-2 with the actual well-killing rate data. The model predicted a minimum pumping rate of 84.5 bbl/min with 7216 psi bottom hole flowing pressure compared with reservoir

pressure 7100 psi which explained in **Figure 5**. In practice, the well blowout was effectively controlled when the pumping rate was increased to 85 bbl/min, and reignited when the pumping rate was reduced to 80 bbl/min.

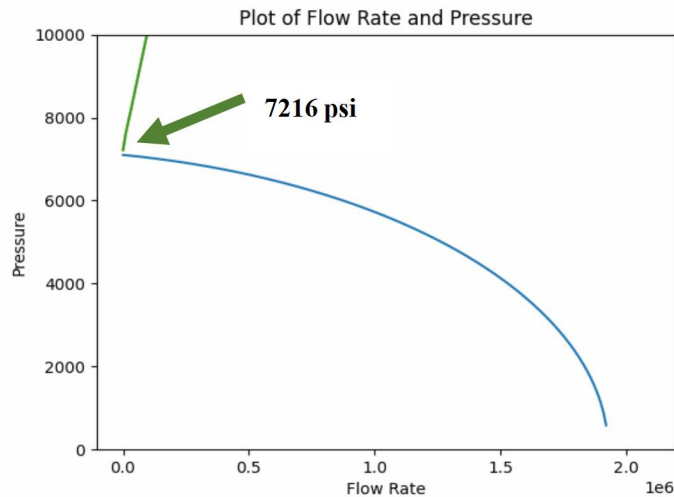


Figure 5—Arun Field well C-II-2 predicted dynamic killing rate.

Gillespie's Case in Workover Well. Gillespie et al. (1990) analyzed a potential dynamic kill for a workover gas well under off-bottom conditions. The study focused on a gas recycling well within an Enhanced Oil Recovery (EOR) project, which was completed with 2-7/8" tubing and snubbed with 1-1/4" coiled tubing to wash sand and dynamically kill the well using a 9.5 lbm/gal sodium chloride (NaCl) solution. Reservoir data are provided in **Table 3**, and the well schematic is shown in **Figure 6**.

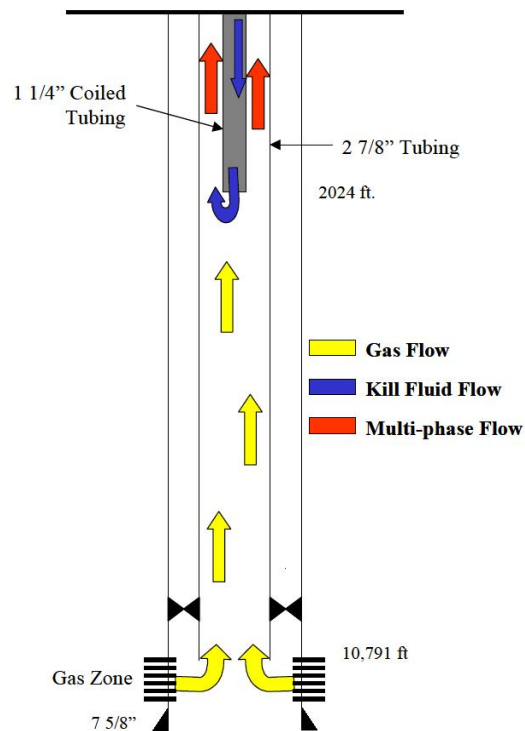
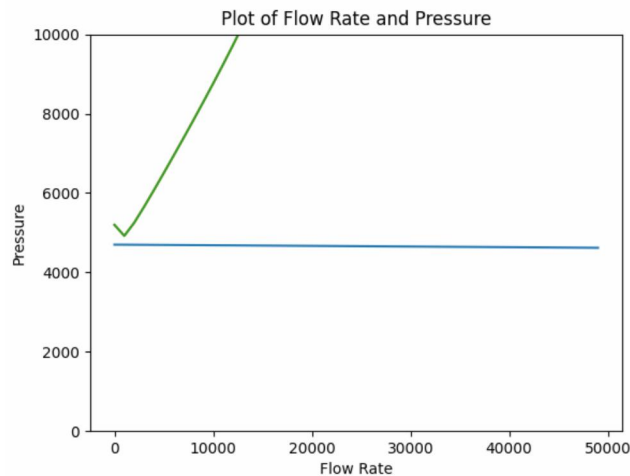


Figure 6—Well completion with kill string (Gillespie et al 1990).

Table 4—Reservoir data (Gillespie et al. 1990).

Parameters	Values
Net thickness, ft	110
Permeability, md	100
Porosity, %	22
Water saturation, %	40
Temperature, °F	172
Reservoir pressure, psi	4,700

The reservoir and wellbore data listed in **Table 4** were used in the model to determine the minimum dynamic kill rate using 9.5 lbm/gal killing fluid with 1-1/4" coiled tubing at a depth of 10,053 ft. The model predicted a killing rate of 0.8 bbl/min, as presented in **Figure 7**, while Gillespie reported a range of killing rates between 0.5 and 1.0 bbl/min (Gillespie et al. 1990).

**Figure 7—Minimum dynamic killing rate in work over well case with 1-1/4" CT at 10053 ft.**

Case Studies

The primary objective of this study is to evaluate the performance of dynamic well control techniques under off-bottom conditions and to identify their limitations. To achieve this, a computer model was developed using the Python programming language to simulate and analyze dynamic killing scenarios for off-bottom gas blowouts.

Arun Field Well C-II-2 Case. A critical aspect of the modeling process is the area below the end of the kill string (Region 2), which was modeled using three different approaches. For the case study of Arun Field well C-II-2, **Figures 8** through **10** illustrate the well inflow/VLP performance with the end of the kill string positioned at 8,000 ft. The killing rate was maintained at 3,850 gal/min, using water as the killing fluid. The modeling approaches included static ZNLH (Figure 8), dynamic ZNLH (Figure 9), and two-phase flow model (Figure 10).

The static ZNLH model resulted in the lowest bottom hole flowing pressure (7,198 psi), whereas the two-phase flow model showed the highest bottom hole flowing pressure (7,478 psi) during well-killing operations. Not accounting for liquid fall-off led to a higher required killing rate (4,390 gal/min) to halt gas influx.

Conversely, when maintaining a fixed bottom hole flowing pressure and performing sensitivity analysis on the killing rate, the static ZNLH model indicated a higher required killing rate (3,850 gal/min), while the two-phase flow model suggested a lower killing rate (3,765 gal/min).

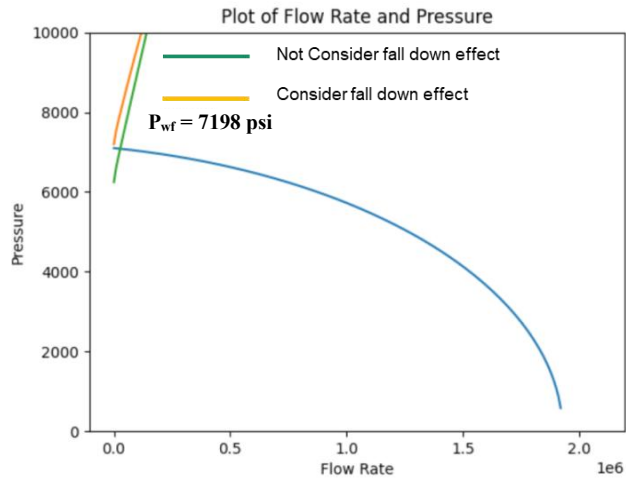


Figure 8—The predicted off-bottom dynamic killing rate of Arun Field well C-II-2 using static ZNLH.

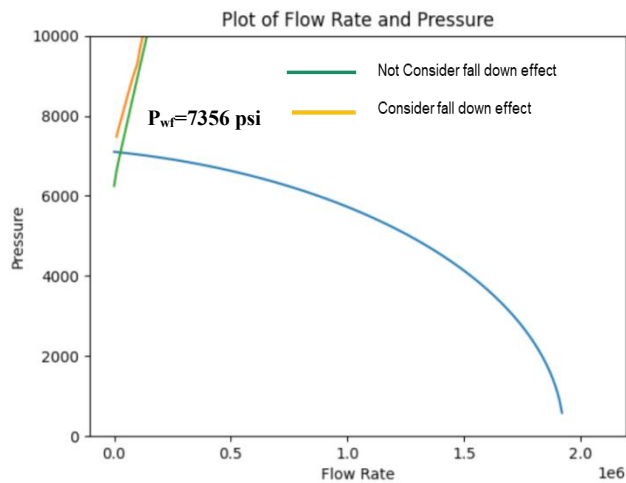


Figure 9—The predicted off-bottom dynamic killing rate of Arun Field well C-II-2 using Dynamic ZNLH.

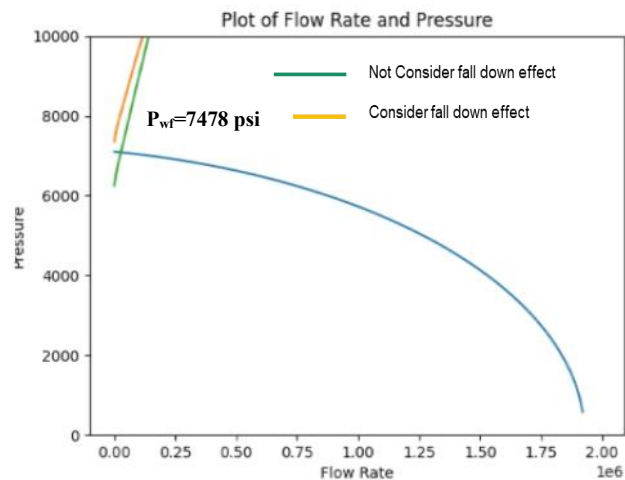


Figure 10—The predicted off-bottom dynamic killing rate of Arun Field well C-II-2 using two phase flow model.

Gillespie’s Case. Figures 11 through 13 illustrate the well inflow/VLP performance for Gillespie's case with the end of the kill string positioned at 2,024 ft. The analysis was conducted at a constant killing rate of 3.7 bbl/min, using water as the killing fluid, and applied static ZNLH, dynamic ZNLH, and two-phase flow model.

The static ZNLH model resulted in the lowest bottom hole flowing pressure (4,909 psi), while the two-phase flow model showed the highest bottom-hole flowing pressure (5,393 psi) during the well-killing operation. Ignoring liquid fall-off led to a higher killing rate (295 gal/min) required to stop gas influx.

Conversely, when maintaining a constant bottom-hole flowing pressure and performing sensitivity analysis on the killing rate, the static ZNLH model indicated a higher required killing rate (155 gal/min), whereas the two-phase flow model suggested a lower killing rate (145 gal/min).

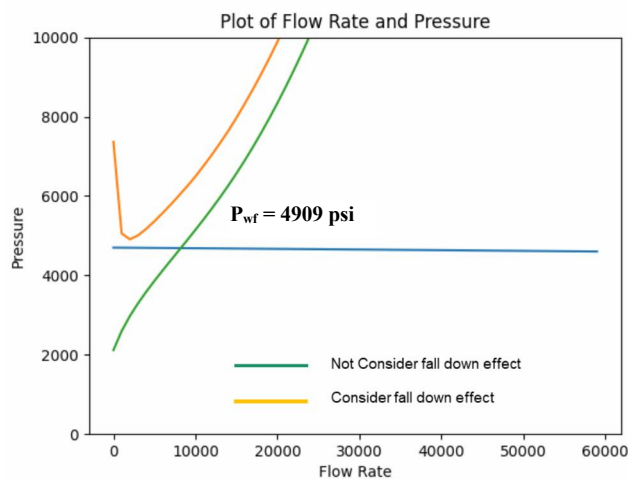


Figure 11—The predicted off-bottom dynamic killing rate of Gillespie’s case using Static ZNLH.

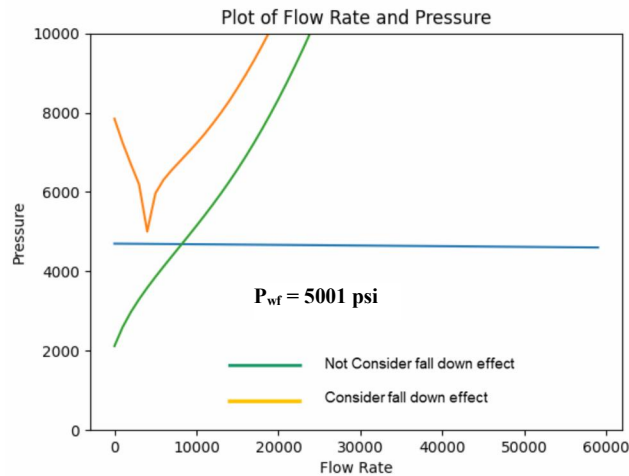


Figure 12—The predicted off-bottom dynamic killing rate of Gillespie's case using dynamic ZNLH.

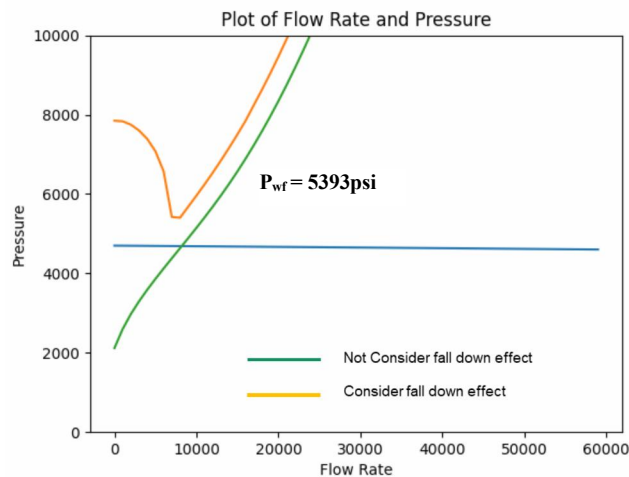


Figure 13—The predicted off-bottom dynamic killing rate of Gillespie's case using using two-phase flow model.

Results and Discussion

One of the objectives of the model is to demonstrate the effect of well operating conditions on the killing parameters, and some of the figures generated by the model illustrate this effect.

Temperature. Temperature has a significant effect on the properties of killing fluids. In the first case study (Arun Field well C-II-2), despite using water as the killing fluid, its properties changed dramatically with depth due to temperature variations. **Figures 14 and 15** illustrate the impact of temperature on water density and viscosity. Water density decreased from 62.5 pounds of cuber foot (PCF) at surface conditions to 59.5 PCF at downhole conditions, while water viscosity decreased from 1.3 CP at the surface to 0.2 CP at total well depth. These changes in water properties will influence the required killing rate, with the effect being even more pronounced if a Non-Newtonian fluid were used as the killing fluid.

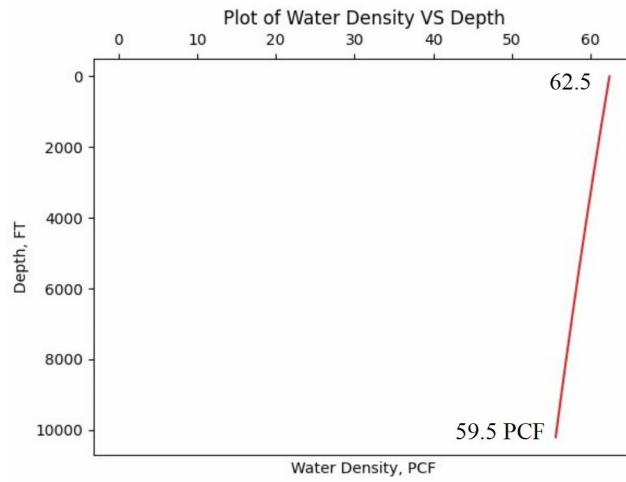


Figure 14—Effect of temperature on water density.

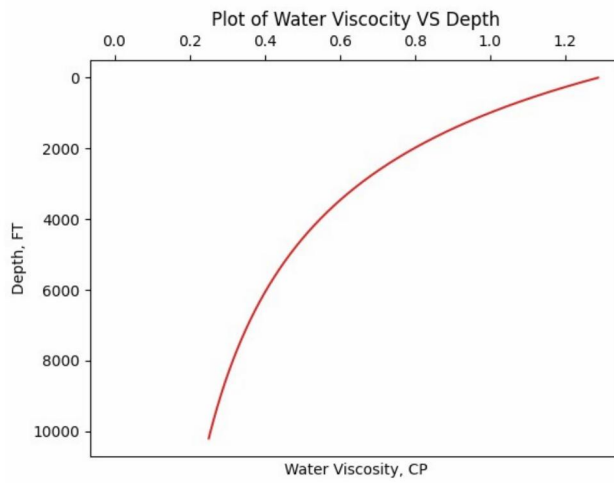


Figure 15—Effect of temperature on water viscosity.

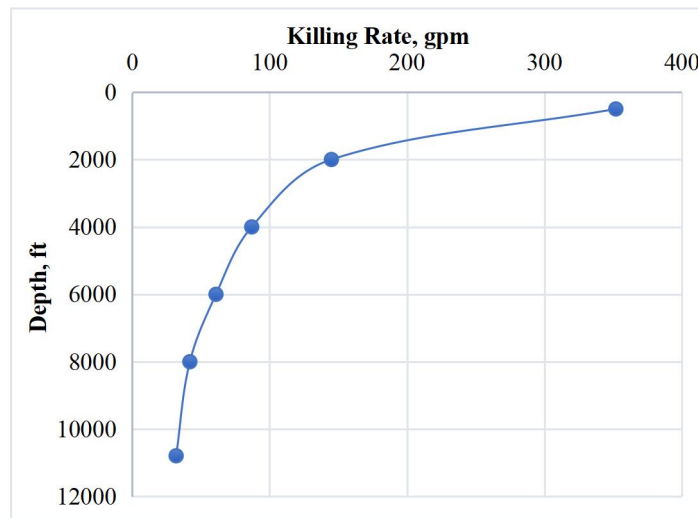


Figure 16—The effect of killing depth on the required kill rate.

Killing Depth. It is evident that the depth of the kill string has a crucial effect on the required kill rate. **Figure 16** illustrates how the depth of the kill string impacts the kill rate in the second case (Gillespie's case). As the depth of the kill string decreases, the required kill rate increases, and follows a logarithmic relationship.

Gas Influx Rate. As previously discussed, the key criterion determining whether the kill fluid will fall to the bottom of the well or move upward with the gas influx is the critical gas velocity (V_c). If the superficial gas velocity (V_{sg}) at the end of the kill string depth exceeds the critical velocity, the kill fluid will fall. **Figures 17 to 20** illustrate V_{sg} and V_c with depth, ranging from the end of the kill string at 2,000 ft to the well's bottom, under different gas influx rates. At low influx rates, the superficial gas velocity is low, resulting in a larger gap between V_{sg} and V_c . As the gas influx rate increases, V_{sg} rises and V_c decreases until they approach a certain limit (influx rate). At this point, V_{sg} becomes lower than V_c , and the kill fluid will no longer fall but instead will flow upward with the kick fluid to the surface.

It is important to note that both velocities decrease with increasing well depth, primarily due to the effect of pressure on gas density. Additionally, the critical gas velocity decreases with increasing gas influx rate because the higher bottom hole pressure results in greater gas density and consequently a lower critical velocity.

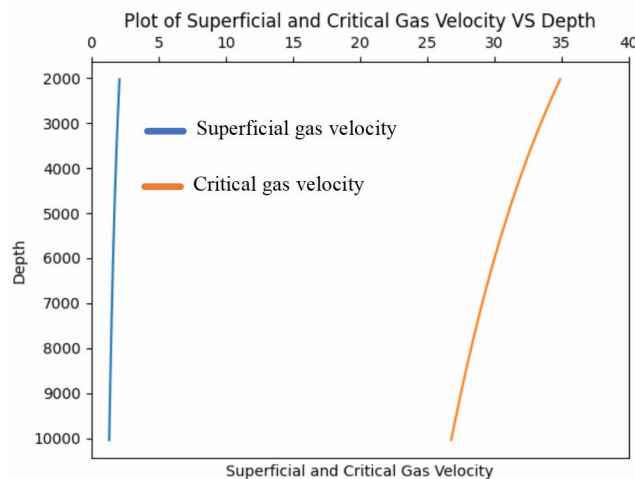


Figure 17— V_c and V_{sg} with depth at gas influx rate of 1 MMscf/d.

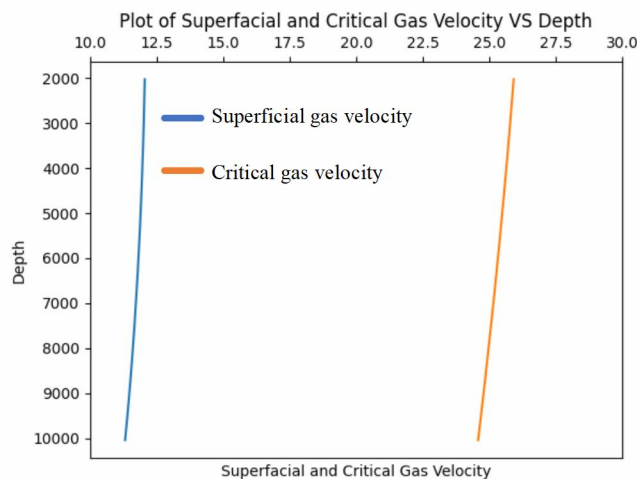


Figure 18— V_c and V_{sg} with depth at gas influx rate of 10 MMscf/d.

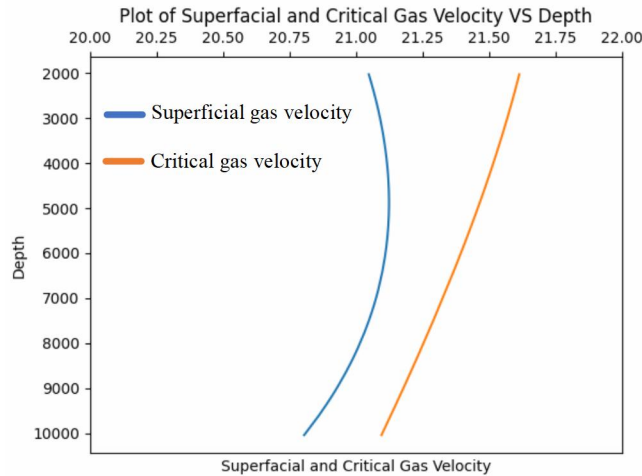


Figure 19— V_c and V_{sg} with depth at gas influx rate of 24 MMscf/d.

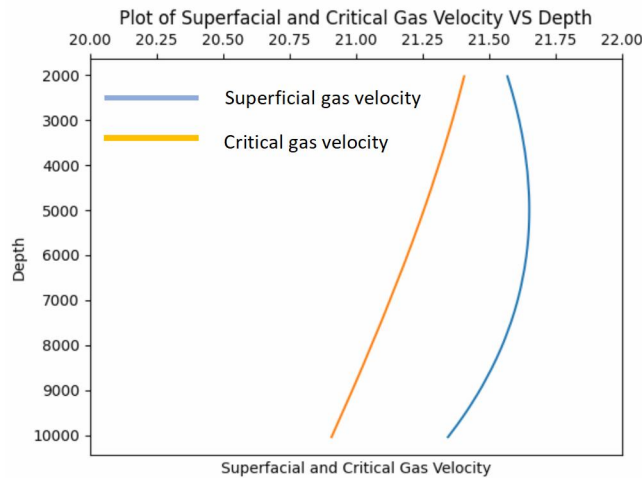


Figure 20— V_c and V_{sg} with depth at gas influx rate of 25 MMscf/d.

Conclusions

In this study, three approaches were employed to develop an optimal model for predicting the dynamic kill technique with the kill string positioned off-bottom. Given the limited practical efforts to model this killing condition, the results obtained can be generalized for modeling off-bottom dynamic killing in gas blowout wells. The constructed model was validated with actual well killing data, and the following conclusions were drawn:

1. The Static Zero Net Liquid Hold-up (ZNLH) model resulted in the lowest bottom hole flowing pressure, indicating a higher kill rate, whereas the two-phase flow model produced the highest bottom hole flowing pressure, reflecting a lower kill rate for well killing operations.
2. Temperature significantly impacts the properties of the killing fluid, even when water is used. Changes in temperature alter the fluid's density and viscosity, which in turn affects the required killing rate.
3. The required kill rate exhibits an inverse logarithmic relationship with the depth of the kill string.
4. Liquid fall-off below the end of the kill string will continue if the superficial gas velocity is lower than the critical gas velocity. As the gas influx rate increases, the superficial gas velocity rises and the critical gas velocity decreases until a certain limit (gas influx rate) is reached, beyond which the liquid fall-off ceases.

5. The critical gas velocity is inversely proportional to the gas influx rate. Higher gas influx rates lead to increased bottom hole pressure and higher gas density, resulting in a lower critical gas velocity.
6. Both superficial and critical gas velocities decrease with increasing well depth due to the effect of pressure on gas density.

Recommendation

For the future work, I would recommend to modify the model to utilize non-Newtonian fluid to be used as killing fluid.

Nomenclature

- a = Well vertical depth, ft;
- C_o = Flow parameter, dimensionless;
- C_p = Heat capacity, $\frac{\text{Btu}}{\text{lbm}\cdot^{\circ}\text{F}}$;
- d_{\max} = Maximum droplet size, ft;
- d_i = Pipe internal diameter, ft;
- D_s = kill string internal diameter, in;
- f = Moody friction factor, dimensionless;
- g = Gravity acceleration, ft/sec^2 ;
- g_G = Geothermal gradient, $^{\circ}\text{F}/\text{ft}$;
- H_l = Liquid hold-up, fraction;
- H_{l0} = Liquid hold-up at ZNLH condition, fraction;
- H_g = Gas void fraction, fraction;
- h = Reservoir thickness, ft;
- J = ft-lbf to btu conversion factor, dimensionless;
- K_d = Sphere drag coefficient, dimensionless;
- k = Reservoir permeability, md;
- l = Total well measured depth, ft;
- L_d = Piper length with annular flow, ft;
- L_p = Pipe length, ft;
- L_R = Relaxation distance parameter, ft^{-1} ;
- P_R = Reservoir pressure, psi;
- P_{wf} = Flowing bottom hole pressure, psi;
- Q_{sc} = Gas flow rate at surface condition, scf/day;
- r_w = Wellbore radius, ft;
- r_e = Reservoir radius, ft;
- T = Temperature, R;
- T_{ann} = Annular fluid temperature, $^{\circ}\text{F}$;
- T_{ei} = Undisturbed formation temperature, $^{\circ}\text{F}$;

Greek:

- v_{scrit} = Critical gas velocity, ft/sec;
 v_s = Slip velocity, ft/sec;
 v_g = Gas velocity, ft/sec;
 v_l = Liquid velocity, ft/sec;
 v_{sg} = Superfacial gas velocity, ft/sec;
 v_{sl} = Superfacial liquid velocity, ft/sec;
 v_{Go} = Gas slip velocity at ZNLH condition, ft/sec;
 v_m = Mixture velocity, ft/sec;
 v_{∞} = Gas rise velocity, ft/sec;
 z = Gas compressibility factor, dimensionless;
 σ = Gas/liquid interfacial tension, lbf/ft;
 α = Deviation angle from vertical, degree;
 μ_g = Gas viscosity, cp;
 μ_l = Liquid viscosity, cp;
 μ_m = Mixture viscosity, cp;
 β = Turbulence factor, ft⁻¹;
 Y_g = Gas specific gravity, dimensionless;
 ρ_l = Density of liquid phase, lb/ft³;
 ρ_g = Density of continuous gas phase, lb/ft³;
 ρ_m = Mixture density, lb/ft³;

Conflicting Interests

The author(s) declare that they have no conflicting interests.

References

- Arpandi, I. A., Ashutosh R. J., Shoham, O., et al. 1996. Hydrodynamics of Two-Phase Flow in Gas-Liquid Cylindrical Cyclone Separators. *SPE Journal* **1**: 427-436.
- Flores-Avila, F. S., Smith, J. R., Bourgoyne, A. T., et al. 2002. Experimental Evaluation of Control Fluid Fallback During Off-Bottom Well Control: Effect of Deviation Angle. Paper presented at the IADC/SPE Drilling Conference, Dallas, Texas, USA, 26-28 February. SPE-74568-MS.
- Flores-Avila, F. S., Smith, J. R., Bourgoyne, A. T. 2003. New Dynamic Kill Procedure for Off-Bottom Blowout Wells Considering Counter-Current Flow of Kill Fluid. Paper presented at the SPE/IADC Middle East Drilling Technology Conference and Exhibition, Abu Dhabi, United Arab Emirates, 20-23 October. SPE-85292-MS.
- Forchheimer, P. 1901. Wasserbewegung durch Boden. *Zeitschrift der Verein Deutscher Ingenieure* **45**:173
- Gillespie, J. D., Morgan, R. F., and Perkins, T. K. 1990. Study of the Potential for an Off-Bottom Dynamic Kill of a Gas Well Having an Underground Blowout. *SPE Drilling Engineering* **5**(3): 215–219. SPE-17254-PA.
- Hasan, A. R. and Kabir, C.S. 2012. Wellbore Heat-transfer Modeling and Applications. *Journal of Petroleum Science and Engineering* **87**:127-136.
- Hasan, A. R. and Kabir, C.S. 2018. Fluid Flow and Heat Transfers in Wellbores (Second Edition). Society of Petroleum Engineers.
- Ikoku, C. U. 1980. Natural Gas Engineering. Tulsa: Penn well Publishing Co.

- Kolla, S. S., Mohan, R. S., and Shoham, O. 2018. Mechanistic Modeling of Liquid Carry-Over for 3-Phase Flow in GLCC© Compact Separators. Paper presented at the ASME 5th Joint US-European Fluids Engineering Division Summer Meeting, Quebec, Canada. 15-20 July.
- Kouba, G. E., MacDougall, G. R., and Schumacher, B. W. 1993. Advancements in Dynamic Kill Calculations for Blowout Wells. *SPE Drilling and Completion* **8**(3): 189-194. SPE-22559-PA.
- Kanshio, S. 2019. An Empirical Correlation for Zero-Net Liquid Flow in Gas-Liquid Compact Separator. *American Journal of Chemical Engineering* **7**(3):81-89.
- Turner, R.G., Hubbard, M.G., and Dukler, A.E. 1969. Analysis and Prediction of Minimum Flow Rate for the Continuous Removal of Liquid from Gas Wells. *Journal of Petroleum Technology* **21**(1): 1475-1482
- Vallejo-Arrieta, V. G. 2002. Analytical Model to Control Off-Bottom Blowouts Utilizing the Concept of Simultaneous Dynamic Seal and Bullheading. PhD dissertation, Louisiana State University, Baton Rouge, Louisiana.
- Yin, B., Ren, M., Liu, S., et al. 2023. Dynamic well killing method based on Y-tube principle when the drill bit is off-bottom. *Engineering Science and Technology, an International Journal* **41**(1): 101385.

Mohamed Yossef, SPE, is a Senior Drilling Engineer started working in 2007 with Belayim Petroleum Company (PETROBEL) in Cairo, Egypt. He worked as drilling well site leader for Saudi Aramco from 2018 to 2020 and from 2022 to 2023, and then as Senior well site leader in Majnoon Oil Field Basra, Iraq. He is a certified well control instructor and assessor for both International Well Control Forum (IWCF) and International Association of Drilling Contractors (IADC). Mr. Yossef has 17 years of drilling operations experience. He specializes in modern water shut off techniques and predicting drilling rate of penetration for hybrid bits. Mr. Yossef holds B.Sc. and M.Sc. degree in petroleum engineering from the Suez University, Egypt.

Adel Salem is a Professor of Petroleum and Mining Engineering, Suez University. Prof. Salem holds a PhD in Petroleum Engineering in 2008 from Leoben University, Austria, and a B.Sc. and M. Sc. from Suez Canal University, Egypt, all in Petroleum Engineering. Prior to Suez University, Prof. Salem served as a full-time Assistant Professor at American University in Cairo (AUC) from 2011 to 2014, and then as an Associate Professor at Petroleum Engineering Department, Future university in Egypt from 2014 to 2016. Prof. Salem has published more than 100 papers in areas such as EOR, characterization of formation damage, nanotechnology applications for EOR and smart drilling fluids, oil shale, well testing, and radial drilling.